IMMUNOLOGY

# Adipose tissue parasite sequestration drives leptin production in mice and correlates with human cerebral malaria

**Pedro Mejia[1]*†, J. Humberto Treviño-Villarreal[1]*†‡, Mariana De Niz[2,3,4§], Elamaran Meibalan[4], Alban Longchamp[1,5,6], Justin S. Reynolds[1], Lindsey B. Turnbull[7], Robert O. Opoka[8], Christian Roussilhon[9], Tobias Spielmann[10], C. Keith Ozaki[5], Volker T. Heussler[3], Karl B. Seydel[11], Terrie E. Taylor[11], Chandy C. John[7], Danny A. Milner[4,12], Matthias Marti[2,4], James R. Mitchell[1]||**



**Circulating levels of the adipokine leptin are linked to neuropathology in experimental cerebral malaria (ECM), but its source and regulation mechanism remain unknown. Here, we show that sequestration of infected red blood cells (iRBCs) in white adipose tissue (WAT) microvasculature increased local vascular permeability and leptin production. Mice infected with parasite strains that fail to sequester in WAT displayed reduced leptin production and protection from ECM. WAT sequestration and leptin induction were lost in CD36KO mice; however, ECM susceptibility revealed sexual dimorphism. Adipocyte leptin was regulated by the mechanistic target of rapamycin complex 1 (mTORC1) and blocked by rapamycin. In humans, although *Plasmodium falciparum* infection did not increase circulating leptin levels, iRBC sequestration, tissue leptin production, and mTORC1 activity were positively correlated with CM in pediatric postmortem WAT. These data identify WAT sequestration as a trigger for leptin production with potential implications for pathogenesis of malaria infection, prognosis, and treatment.**

## INTRODUCTION

Cerebral malaria (CM) is a life-threatening complication of infection with *Plasmodium falciparum* parasites manifesting with intracerebral hemorrhages, brain edema, coma, and death (*1*–*3*). Children under the age of 5 with little or no previous exposure to *P. falciparum* infection are most vulnerable to CM (*4*), but it is currently impossible to predict which infected patients will progress to CM (*5*). Once the deadly syndrome has developed, no efficient treatment exists to reduce mortality and long-term neurologic disabilities even after successful elimination of circulating blood-stage parasites with antimalarial chemotherapy. While exact molecular mechanisms remain unclear, the disease appears to be the result of a complex interplay between infected red blood cells (iRBCs) and local and systemic host immune responses (*6*–*8*). On a histological level, neurovascular perturbations include increased blood-brain barrier (BBB) permeability, leukocyte infiltration, platelet activation (*9*), and dysregulation of the coagulation system in brain endothelium (*2*, *10*).

Sequestration of iRBCs via cytoadherence to the microvasculature is a hallmark of severe malaria across multiple *Plasmodium* species (*11*). iRBC sequestration, which represents a strategy by the parasite to evade host immune clearance by the spleen, can lead to pathology via endothelial cell activation and/or mechanical obstruction of blood flow. In humans, sequestration in the brain microvasculature is a defining feature of CM neuropathogenesis (*12*, *13*); but sequestration also occurs widely in organs and tissues outside of the brain. Histopathological analyses of iRBC sequestration in postmortem samples from *P. falciparum*–infected children who died from CM or other causes (*2*, *14*–*16*) show that iRBCs sequester across most of the organs analyzed, including the gastrointestinal tract and the subcutaneous white adipose tissue (ScWAT) (*2*, *15*, *16*). iRBCs express adhesion molecules including the variable *P. falciparum* erythrocyte membrane protein 1 (*Pf*EMP1) (*17*, *18*) that cytoadhere to host endothelial cell receptors such as intercellular adhesion molecule–1 (ICAM-1), endothelial protein C receptor (EPCR), and the scavenger receptor/fatty acid transporter CD36 (*19*–*21*). In brain endothelium, ICAM-1 is activated by local or systemic proinflammatory cytokines (*22*), while CD36 is expressed in both endothelial and parenchymal cells in other tissues with high levels of fatty acid metabolism including in WAT and lung, but not in brain (*23*).

In rodent models of experimental CM (ECM) using *Plasmodium berghei* ANKA (*Pb*A) in susceptible hosts including C57BL/6 mice, sequestration of iRBCs also occurs in multiple tissues including lung and adipose, both of which are largely dependent on CD36, although the corresponding ligand on *Pb*A-infected RBCs remains to be defined (*24*, *25*). Parasites also accumulate in brain, but whether this is due to CD36-independent cytoadherence and sequestration in the brain microvasculature (*26*) or the result of BBB dysfunction

[1]Department of Genetics and Complex Diseases, Harvard T. H. Chan School of Public Health, Boston, MA, USA. [2]Wellcome Centre for Molecular Parasitology, Institute of Infection, Immunity and Inflammation, University of Glasgow, Glasgow, UK. [3]Institute of Cell Biology, University of Bern, Bern, Switzerland. [4]Department of Immunology and Infectious Diseases, Harvard T. H. Chan School of Public Health, Boston, MA, USA. [5]Department of Surgery and the Heart and Vascular Center, Brigham and Women's Hospital and Harvard Medical School, Boston, MA, USA. [6]Department of Vascular Surgery, Centre Hospitalier Universitaire Vaudois and University of Lausanne, Lausanne, Switzerland. [7]Department of Pediatric Infectious Diseases, Indiana University School of Medicine, Indianapolis, IN, USA. [8]Department of Pediatrics and Child Health, Makerere University, Kampala, Uganda. [9]Department of Genomes and Genetics, Pasteur Institute, Paris, France. [10]Bernhard Nocht Institute for Tropical Medicine, Hamburg, Germany. [11]Department of Osteopathic Medical Specialties, Michigan State University, East Lansing, MI, USA. [12]American Society for Clinical Pathology, Chicago, IL, USA.
*Corresponding author. Email: mejia.jp@gmail.com (P.M.); jhumbertotrevino@imagenehealth.com (J.H.T.-V.)
†These authors contributed equally to this work.
‡Present address: Endocrinology Service, University Hospital José Eleuterio Gonzalez and School of Medicine, Universidad Autónoma de Nuevo León, Monterrey, Mexico.
§Present address: Instituto de Medicina Molecular, Faculdade de Medicina da Universidade de Lisboa, Avenida Professor Egas Moniz, 1649-028 Lisboa, Portugal.
||Deceased.

remains a matter of debate. Despite conservation of sequestration in peripheral tissues such as adipose and lung, relevance to ECM neuropathology remains questionable in large part because CD36KO mice, which fail to support CD36-dependent sequestration in major sequestering tissues, still succumb to ECM (*11*, *24*, *25*).

In addition to energy storage, adipose tissue and adipocytes are metabolically active and capable of secreting a myriad of bioactive molecules including cytokines and hormones, collectively known as adipokines, which link metabolism, inflammation, and immunity (*27*, *28*). One of these adipokines, leptin, has central effects promoting food intake and energy expenditure, as well as peripheral effects promoting immune and endothelial cell activation (*29*–*31*). Leptin is increased upon *Pb*A infection and required for ECM neuropathology via induction of T cell effector functions and migration capacity (*32*, *33*). Enforced restriction of food intake in the first 3 days of blood-stage infection can ameliorate ECM symptoms without affecting peripheral parasitemia, in part, by blunting the increase in circulating leptin (*33*). However, neither the trigger for leptin secretion in the ECM model nor the potential role of leptin in CM pathogenesis in humans has been evaluated.

Here, we tested the hypothesis that iRBC sequestration specifically in WAT is a major driver of increased leptin production in ECM. We found that leptin protein expression increased in multiple WAT depots of wild-type (WT) C57BL/6 mice infected with blood-stage *Pb*A and that this correlated with increased vascular permeability in this tissue. Using both parasite and host mutants, we found a correlation between iRBC sequestration in WAT and increased host leptin production, with the nutrient sensor mechanistic target of rapamycin complex 1 (mTORC1) implicated in specific up-regulation of leptin mRNA and protein expression in adipocytes. Last, changes in parasite sequestration, mTORC1 activity, and local leptin expression in pediatric postmortem adipose samples from CM patients suggest evolutionary conservation of the phenomenon.

## RESULTS

### Sequestration of iRBCs in WAT promotes tissue vascular permeability and leptin production

We evaluated parasite sequestration in different tissues of C57BL/6 mice over a time course after infection with luciferase-expressing *Pb*A (BL6-*Pb*A) parasites (*33*). Using in vivo imaging, sequestration was detectable by day 1 and increased in intensity until day 6, coinciding with the presence of severe neurological symptoms and onset of mortality (Fig. 1A). Assessment on day 6 using a more quantitative approach in organ extracts following intracardiac perfusion revealed that parasite accumulation was highest on a per milligram tissue basis in lung, spleen, and WAT, including perigonadal (Pg) and subcutaneous depots (Fig. 1B). Together, these tissues accounted for >90% of sequestered parasite burden (Fig. 1B). Consistent with in vivo imaging, substantial Pg and ScWAT parasite sequestration were detectable by day 3 and increased at least up to day 6 after infection (Fig. 1C). Histological examination of ScWAT of C57BL/6 or ubiquitin C (UBC)–green fluorescent protein (GFP) C57BL/6 reporter mice on day 6 of infection revealed intravascular localization of iRBCs rather than direct contact with adipocytes (Fig. 1D). An absence of leukocyte infiltration was also noted in hematoxylin and eosin (H&E)–stained sections of this tissue (Fig. 1D). Intravenous injection of iRBCs harboring mature parasite stages resulted in WAT accumulation detectable 3 hours after injection into naïve mice (Fig. 1E), suggesting that parasite sequestration in this tissue is independent of any preexisting local or systemic inflammation.

Circulating leptin increases upon infection and is required for full penetrance of neuropathology and mortality in the ECM model (*33*). However, multiple cells secrete this adipokine, and thus, the cellular source in the context of ECM is unknown. Because WAT is a major source of leptin production, we looked at local leptin expression by immunofluorescence in WAT sections obtained from perfused mice before infection (day 0) and on days 4, 5, and 6 after infection. We observed a progressive increase in local leptin expression in Pg and ScWAT during the course of infection of ECM mice (Fig. 1, F and G), with kinetics similar to that of serum leptin (*33*).

To determine how iRBC sequestration in the WAT vasculature could promote leptin production/secretion by adipocytes in the absence of direct interaction between iRBCs and adipocytes, we examined vascular permeability over a time course after infection via intravenous dextran administration (Fig. 1H). Leakage of dextran (70 kDa), indicative of increased vascular permeability in WAT, was detected by day 5 of infection. This correlation between WAT parasite accumulation and tissue leptin expression suggests WAT as a major contributor of circulating leptin and local parasite sequestration as the trigger for leptin production.

### Sequestration of iRBCs in WAT is required for leptin production

To assess the potential role of WAT iRBC sequestration in leptin production and correlation with neuropathology, we tested three different luciferase-expressing parasites with altered sequestration and/or virulence relative to WT *Pb*A parasites. Parasites lacking genes encoding the schizont membrane–associated cytoadherence (ΔSMAC) protein or skeleton-binding protein 1 (ΔSBP1) exhibit reduced peripheral parasitemia levels and CD36-dependent lung and WAT sequestration and fail to induce ECM neuropathology (*34*, *35*). *P. berghei* K173 (*Pb*K173) iRBCs also accumulate more slowly and fail to induce ECM (*36*), although sequestration profiles have not been reported. We observed reduced peripheral parasitemias with *Pb*AΔSBP1, *Pb*AΔSMAC, and *Pb*K173 (Fig. 2, A and B), as well as reduced iRBC sequestration on day 6 after infection in PgWAT in ScWAT (Fig. 2C). This correlated with significantly reduced iRBC accumulation in brain (Fig. 2D), lower levels of serum leptin (Fig. 2E), and improved survival (Fig. 2F) relative to C57BL6 mice infected with WT *Pb*A. By day 6 after infection, lung sequestration was significantly elevated in one parasite line (*Pb*K173) and reduced in another (ΔSMAC) and thus failed to correlate with leptin levels or survival.

We next tested a model of reduced sequestration due to genetic changes in the host. As previously reported (*11*, *24*), female CD36KO mice on a C57BL/6 genetic background infected with *Pb*A showed a significant reduction in peripheral parasitemia (Fig. 2, A and B) and reduced iRBC sequestration in PgWAT, ScWAT, and lung relative to WT littermates (Fig. 2C) but still exhibited signs of ECM neuropathology including parasite accumulation in brain on day 6 of infection that was not significantly different than control females (Fig. 2D). This was likely due to breakdown of BBB function as evidenced by increased Evan's blue staining in brain (Fig. 2G). Mortality occurred on a similar time frame (days 6 to 10 after infection) and with slightly less penetrance than control females, although the difference was not statistically significantly (log-rank test, $P = 0.08$; Fig. 2F).

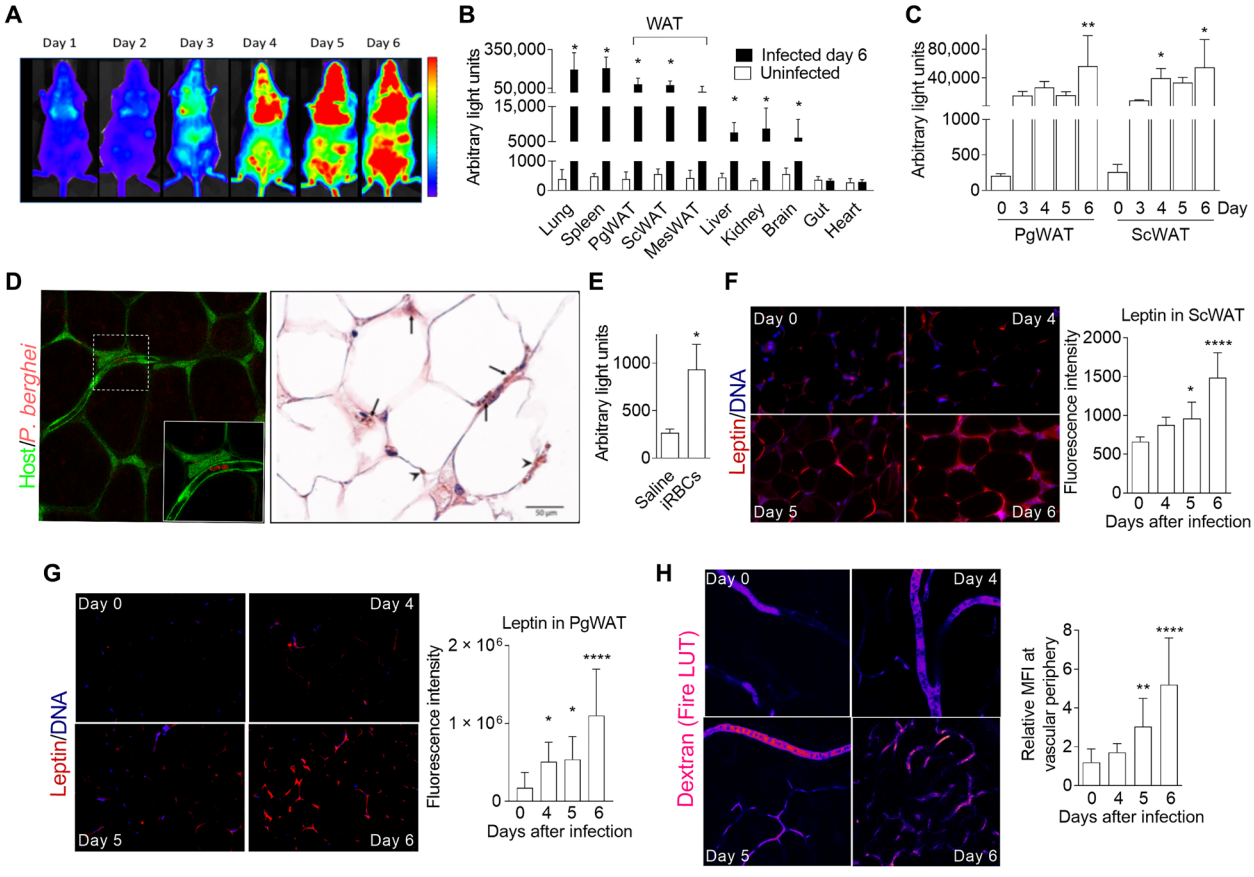


**Fig. 1. *Pb*A iRBC sequestration in WAT correlates with leptin production in the ECM model.** (**A**) Time course of luciferase-expressing *Pb*A parasites in live C57BL6 mice (BL6-*Pb*A) using in vivo imaging from days 1 to 6 after infection. (**B**) Quantitation of sequestration of luciferase-expressing transgenic *Pb*A parasites in the indicated tissue from infected C57BL/6 mice versus naïve controls ($n = 3$ per group) measured ex vivo in organ homogenates after perfusion on day 6 after infection; Mann-Whitney test between groups within a given organ/tissue. (**C**) Sequestration kinetics of luciferase-expressing *Pb*A parasites in Pg and ScWAT homogenates harvested after perfusion on the indicated day after infection ($n = 3$ per time point; Kruskal-Wallis test with Dunn's multiple comparisons test on the indicated day versus day 0). (**D**) Sequestration of iRBCs in WAT microvasculature of *Pb*A-infected mice on day 6 after infection by fluorescence microscopy with mCherry-expressing *Pb*A (red to visualize intact parasites) in UBC promoter–driven GFP C57BL/6 mice (ubiquitous green expression to visualize host cells) in PgWAT (left) or H&E in ScWAT in WT C57BL/6 mice (right). (**E**) RBCs harboring mature parasites accumulate rapidly in WAT. Sequestration was measured ex vivo in PgWAT homogenates harvested following perfusion 3 hours after intravenous injection of saline vehicle (saline) or $5 \times 10^6$ iRBCs; $n = 4$ mice per group; Mann-Whitney test. (**F** and **G**) Representative images of leptin expression and quantitation of fluorescence intensity in ScWAT (F) and PgWAT (G) of *Pb*A-infected C57BL/6 on days 0, 4, 5, and 6 after infection; $n = 10$ microscopic fields per mouse tissue with two mice per group; Kruskal-Wallis test with Dunn's multiple comparisons test against day 0. (**H**) Representative images of FITC-labeled dextran (70 kDa) in WAT 2 hours after intravenous injection into mice on the indicated day after infection; quantitation of dextran Fire LUTs (lookup tables) outside of vessel relative to day 0 at right; Kruskal-Wallis test with Dunn's multiple comparisons test against day 0. All data are expressed as mean ± SD; $^*P < 0.05$, $^{**}P < 0.01$, $^{***}P < 0.001$, and $^{****}P < 0.0001$. MFI, mean fluorescence intensity.

The response to *Pb*A infection in male CD36KO mice was very similar to female CD36KO mice in terms of reduced peripheral parasitemia (Fig. 2, A and B) and reduced sequestration in PgWAT and ScWAT with a tendency toward reduction in lung (Fig. 2C). However, unlike females, males were almost completely protected against ECM neuropathology, including significantly reduced iRBC accumulation in brain on day 6 of infection (Fig. 2D), reduced Evan's blue staining consistent with maintenance of BBB function (Fig. 2G), and highly significant improvement in survival relative to either WT males (which did not significantly differ from WT females in any of the abovementioned parameters) or CD36KO females (log-rank test, $P < 0.0001$) (Fig. 2F).

Consistent with our model, reduced WAT sequestration correlated with a significant reduction in circulating leptin on day 6 after infection in both male and female CD36KO mice (Fig. 2E). However, sexual dimorphisms in leptin levels before and after infection were also observed. In naïve mice (Fig. 2H, green triangles), leptin levels were significantly reduced in female versus male CD36KO mice. Furthermore, while leptin levels tended to increase upon infection in WT females and males (Fig. 2, H and I), leptin levels were significantly reduced upon infection specifically in CD36KO males relative to WT males, while in females they remained low.

Together, these data suggest that CD36-dependent sequestration of iRBC in WAT, but not lung, underlies the increase in circulating leptin levels. They also revealed ECM susceptibility and changes in leptin levels upon infection as sexually dimorphic traits in mice lacking CD36.

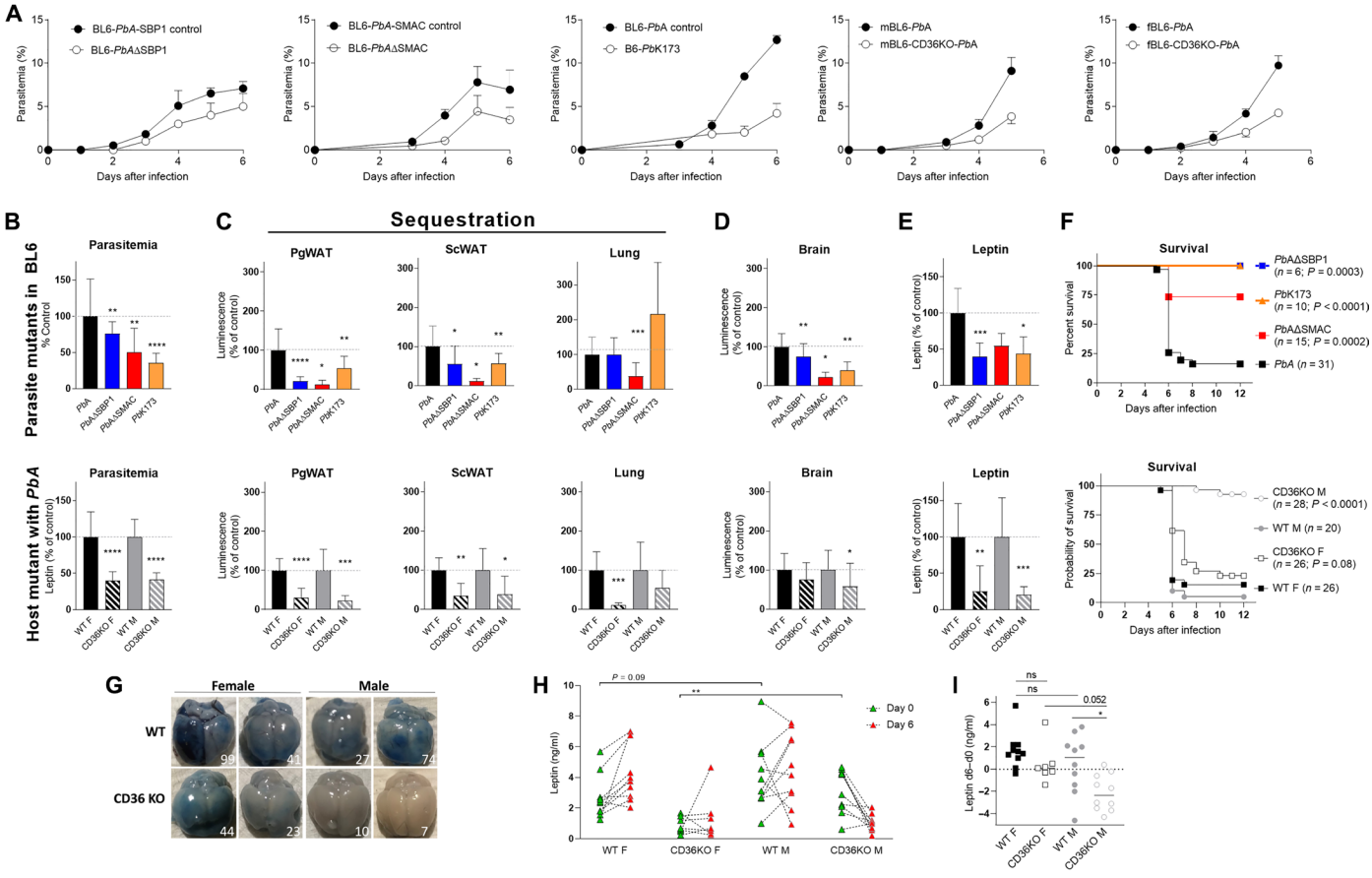


**Fig. 2. Parasite sequestration in WAT is required for systemic leptin production and mortality.** (**A**) Percent peripheral parasitemia over time grouped by experiment with corresponding controls as indicated, including SBP1-deficient versus parental WT *Pb*A into WT female BL6 ($n = 10$ per group), SMAC-deficient versus parental WT *Pb*A into WT female BL6 ($n = 5$ per group), *Pb*K173 versus WT *Pb*A into WT female BL6 ($n = 5$ to 6 per group), and WT *Pb*A into male or female WT ($n = 13$ to 16 per group) versus male (M) or female (F) CD36KO ($n = 16$ to 17 per group) BL6 mice. (**B**) Peripheral parasitemia on day 6 (above) or day 5 (below) expressed as a percent of the corresponding sex-matched control. (**C** to **E**) Day 6 organ-specific sequestration (C), brain parasite accumulation (D), and serum leptin (E) expressed as a percentage of the control for that particular experiment as indicated in (A) and grouped by parasite (top row) or host (bottom row) mutant/strain. Statistics in (B) to (E) were performed using unpaired *t* tests with Welch's correction or Mann-Whitney tests between mutants/strains and their corresponding host/strain control. (**F**) Kaplan-Meier survival curves of mice from the indicated experimental groups infected on day 0, including the number in each group and the log-rank statistic relative to sex-matched BL6-*Pb*A controls. (**G**) Evan's blue–stained brains of the indicated sex/genotype on day 6 after infection; white numbers indicate quantification of Evan's blue after extraction in micrograms per gram of tissue. (**H** and **I**) Circulating leptin levels of the indicated sex/genotype presented as absolute values before (day 0, green triangles) and on day 6 after infection (red triangles), with dotted lines representing individual animals (H) or as differences between circulating leptin on day 6 and day 0 (I); one-way analysis of variance (ANOVA) with Sidak's multiple comparisons tests as indicated. All data are expressed as mean ± SD; $^{*}P < 0.05$, $^{**}P < 0.01$, $^{***}P < 0.001$, and $^{****}P < 0.0001$. ns, not significant; d0, day 0; d6, day 6.

## Sequestered iRBCs stimulate adipocyte leptin production via cell-autonomous mTORC1 activation

Next, we investigated molecular mechanisms controlling leptin production upon parasite sequestration in WAT. The role of the nutrient/energy sensor mTORC1 in posttranscriptional regulation of leptin production in cultured adipocytes has been suggested based on inhibition with the macrolide antibiotic rapamycin (*37*). We thus first measured phosphorylation status of the indirect mTORC1 target S6 in PgWAT by immunofluorescence across multiple time points following infection of C56BL/6 mice with *Pb*A. Increased S6 phosphorylation was observed on days 4 to 6 (Fig. 3A). Western blotting revealed a similar increase in phosphorylation of the direct mTORC1 target, S6 kinase (S6K), in WAT from female and male BL6-*Pb*A mice on day 6 after infection relative to naïve mice (Fig. 3, B and C). This increase in phospho-S6K was mitigated in female WT mice treated with rapamycin or infected with *Pb*A-ΔSMAC (Fig. 3B), as well as in male CD36KO infected with *Pb*A (Fig. 3C), and thus correlated with reduced iRBC WAT sequestration (Fig. 2B).

Treatment of *Pb*A-infected female C57BL6 mice with rapamycin, which offered complete protection from ECM-associated mortality without affecting peripheral parasitemia, also reduced circulating leptin levels (Fig. 3D). To investigate cell-autonomous effects of mTORC1 on adipocyte for leptin production, we knocked down the mTORC1 inhibitor TSC2 in primary adipocytes using adenoviral short hairpin RNA (shRNA). Leptin gene expression and protein secretion were both significantly increased in shTSC2-infected adipocytes compared to control cells infected with scrambled shRNA construct (Fig. 3E). Expression of adiponectin, an adipokine produced exclusively by adipocytes, was not affected by shTSC2 infection. Primary fibroblasts, which do not express adipokines at high

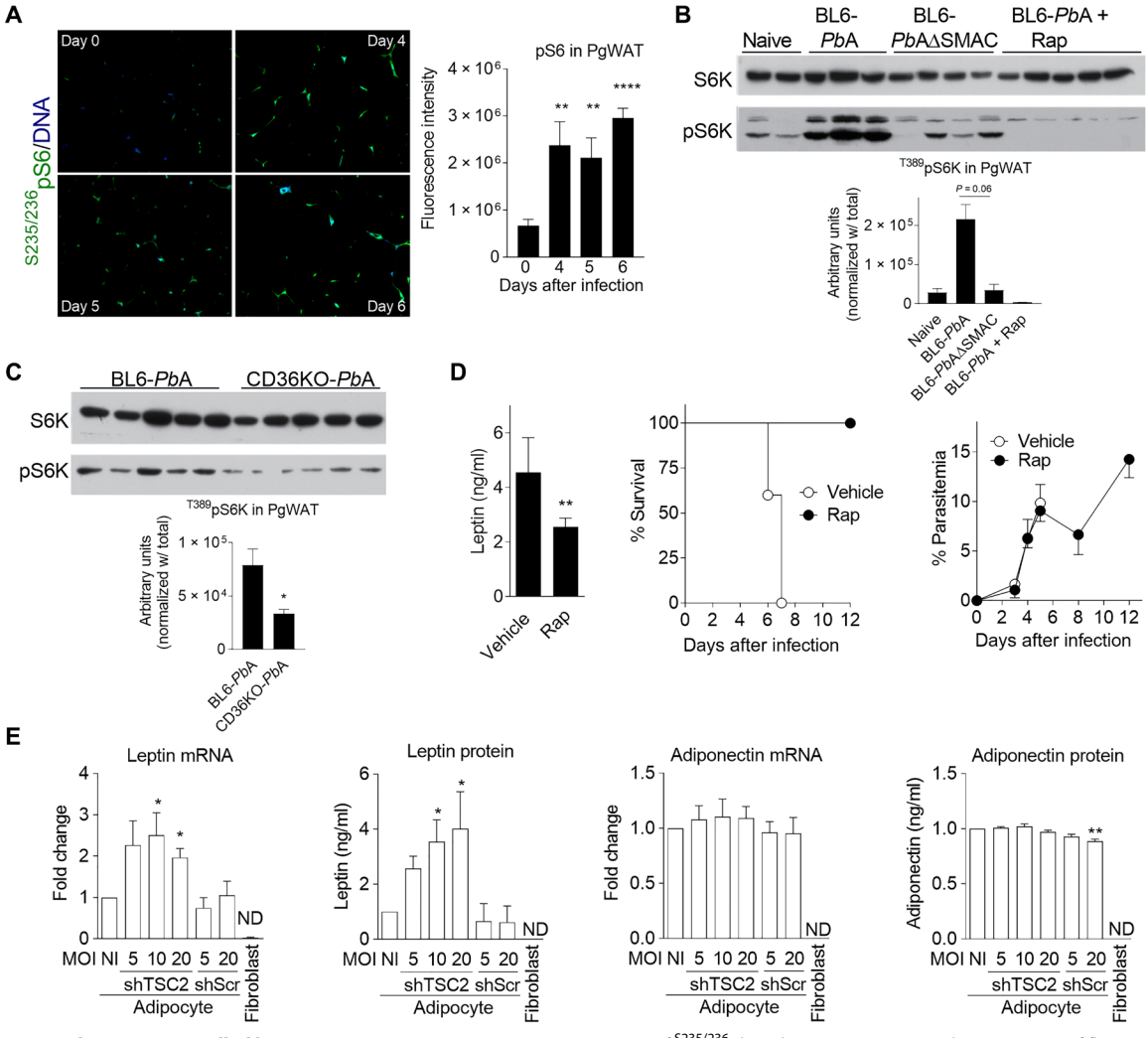


**Fig. 3. WAT leptin production is controlled by mTORC1 activity.** (**A**) Representative images of $^{S235/236}$phospho-S6 expression and quantitation of fluorescence intensity in PgWAT of female *Pb*A-infected C57BL/6 on days 0, 4, 5, and 6 after infection; 5 to 10 fields were imaged in at least three sections from two different animals in each group; $^{**}P < 0.01$ and $^{****}P < 0.0001$, Kruskal-Wallis test with Dunn's multiple comparisons test relative to day 0. (**B**) Immunoblots of total and $^{T389}$phospho-S6K in PgWAT obtained from C57BL/6 female mice that were uninfected (naïve) or from the indicated mouse-parasite experimental group on day 6 after infection or *Pb*A-infected and injected with rapamycin (Rap; 1 mg/kg) 2 days earlier, with quantitation below; Mann-Whitney test as indicated. (**C**) Immunoblots of total and $^{T389}$phospho S6K in PgWAT from male CD36KO and WT littermates infected with *Pb*A with quantitation below; Mann-Whitney test. (**D**) Serum leptin levels on day 6 after infection (left, Mann-Whitney test), survival curves (middle, log-rank test $P = 0.0031$), and peripheral parasitemia (right) of female BL6-*Pb*A mice treated with vehicle or rapamycin (1 mg/kg) on day 4 after infection; $n = 5$ per group. (**E**) Leptin and adiponectin gene expression and protein secretion into the media in primary adipocyte cultures infected with adenovirus expressing shRNAs targeting the mTORC1 inhibitor TSC2 (shTsc2) or control scrambled RNA (shScr) at the indicated multiplicity of infection (MOI). Fibroblasts were used as negative controls. NI, not infected; ND, not detected. Kruskal-Wallis test with Dunn's multiple comparisons test versus NI. All data are expressed as mean ± SD. $^{*}P < 0.05$, $^{**}P < 0.01$, and $^{****}P < 0.0001$.

levels, were used as negative controls (Fig. 3E). Together, these data suggest that mTORC1 activation in adipocytes likely contributes to increased leptin expression upon *Pb*A sequestration in WAT.

## Parasite sequestration, mTORC1 phosphorylation, and local leptin production in human subcutaneous adipose tissue correlate with CM mortality without increased circulating leptin

To assess the relevance of our findings in the mouse ECM model to humans, we explored the relationship between WAT parasite sequestration, leptin production, and pathology in samples obtained from human pediatric CM cases versus controls. We first measured plasma leptin levels in CM cases from Cambodia and Senegal versus uninfected controls from France and Senegal. Contrary to our results in mouse models, no significant differences in the levels of circulating leptin were detected among the groups (Fig. 4A). These results were confirmed in independent cohorts of well-defined cases of CM from Uganda and Malawi versus uninfected, uncomplicated malaria and severe malaria anemia cases (Fig. 4B). We did not find any sexual dimorphism in the incidence of CM either in the literature or in this dataset.

We next assessed leptin production on a histological level in ScWAT from previously characterized fatal CM versus *P. falciparum*–infected non-CM cases from Malawi. As previously reported (*2*, *15*), extensive

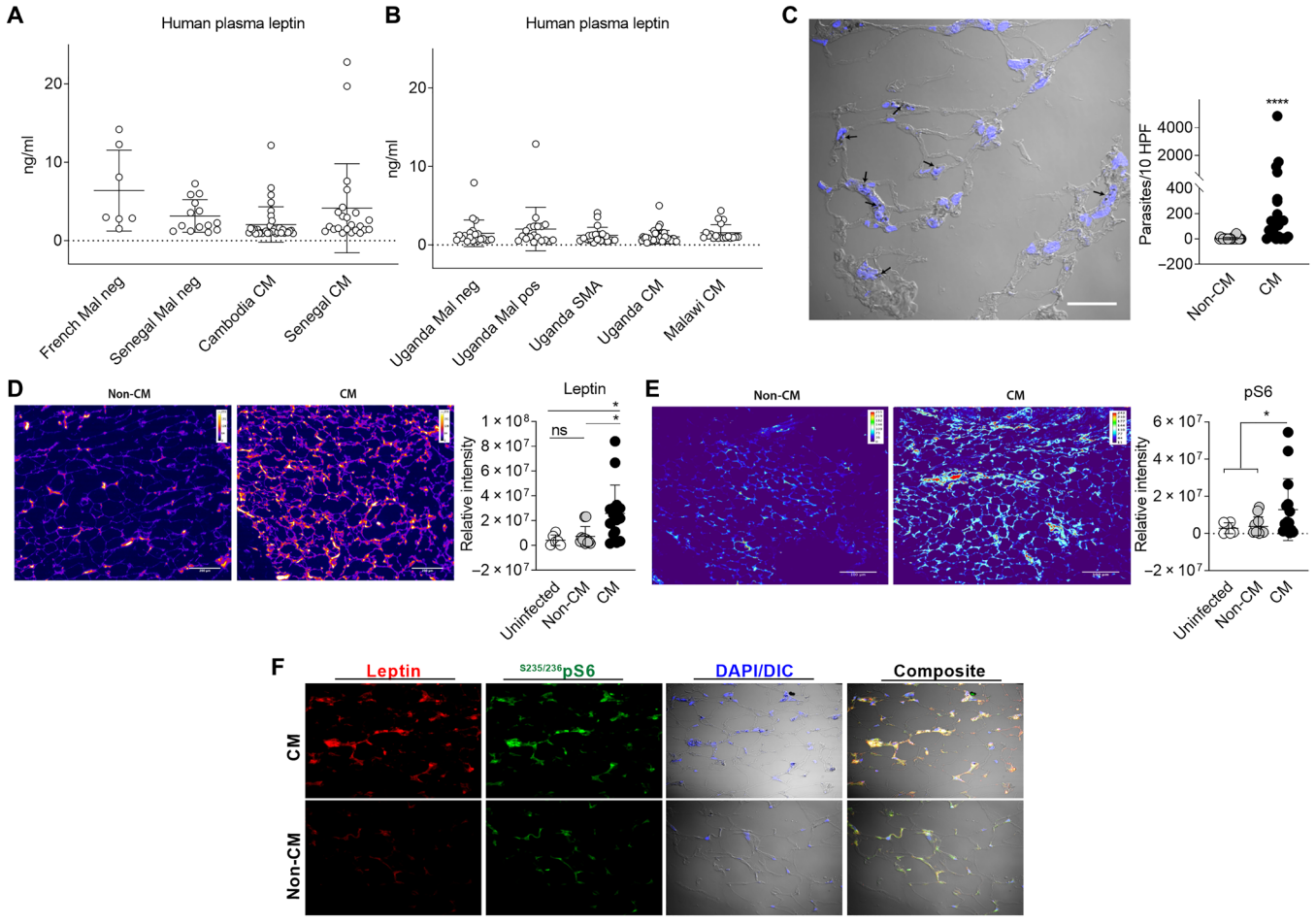


**Fig. 4. Positive correlation between ScWAT parasite sequestration, leptin expression, and mTORC1 activation in human CM.** (**A** and **B**) Human plasma leptin levels measured by ELISA in the following groups: (A) CM cases from Cambodia and Senegal, with uninfected controls (Mal neg) from Senegal or France; (B) CM cases from Uganda and Malawi, as well as SMA, uncomplicated malaria (Mal pos) and uninfected controls from Uganda (Mal neg); Kruskal-Wallis test versus uninfected controls. (**C**) Representative differential interference contrast (DIC) image with 4′,6-diamidino-2-phenylindole (DAPI) counterstain of ScWAT from a fatal case of CM. DAPI stains endothelial and adipocyte nuclei as well as *P. falciparum* iRBCs sequestered in the microvasculature; dark hemozoin pigment (arrows) marks iRBCs. Right: Quantification of iRBC sequestration in ScWAT sections from fatal CM ($n = 24$) and *P. falciparum*–infected non-CM cases ($n = 22$). Each dot represents the median of the number of iRBCs per 10 high-power fields (HPF); Mann-Whitney test. (**D**) Representative thermal-scale images (magnification, ×10) and quantification of relative intensity of leptin protein levels in ScWAT from postmortem *P. falciparum*–infected non-CM ($n = 11$) and CM ($n = 15$) cases relative to uninfected controls ($n = 6$); Kruskal-Wallis test with Dunn's multiple comparisons tests as indicated. (**E**) Representative thermal-scale images (magnification, ×20) and quantification of relative intensity of $^{S235/236}$phospho-S6 protein levels in ScWAT from uninfected ($n = 6$), *P. falciparum*–infected non-CM ($n = 11$), and CM ($n = 15$) cases; Mann-Whitney test. (**F**) Representative confocal microscopy images of ScWAT from *P. falciparum*–infected non-CM and CM cases showing leptin (red), $^{S234/235}$pS6 (green), parasite [DAPI/DIC and hemozoin (black)], and colocalization (composite). All data are expressed as mean ± SD; $^*P < 0.05$ and $^{****}P < 0.0001$.

accumulation of *P. falciparum* iRBCs specifically in ScWAT was detected in CM cases but were virtually absent in non-CM cases (Fig. 4C). Leptin levels were then assessed by immunofluorescence staining in a subset of *P. falciparum*–infected non-CM and CM cases, using uninfected American WAT samples as controls. Notably, leptin expression in ScWAT, expressed as relative fluorescence intensity, was significantly increased in CM cases relative to non-CM and uninfected controls (Fig. 4D). Consistent with results obtained in mice, phosphorylation of the indirect mTORC1 target S6 was significantly elevated in ScWAT from CM cases compared to *P. falciparum*–infected non-CM and uninfected controls (Fig. 4E), with substantial colocalization of leptin and phospho-S6 in regions of parasite accumulation (Fig. 4F). Together, these results suggest evolutionary conservation of a link between *Plasmodium*-infected RBC sequestration in WAT, activation of mTORC1, and increased local leptin expression in both humans and mice.

## DISCUSSION

Sequestration of *Plasmodium*-infected RBCs in WAT was first described decades ago in humans and nonhuman primates (*38*). Although *Plasmodium* species are thought to remain within the adipose microvasculature, at least two other parasites—*Trypanosoma cruzi*, the causative agent of Chagas disease, and *Trypanosoma brucei*, the causative agent of African sleeping sickness—localize within and between adipocytes, respectively, in their mammalian hosts (*39*). Several

potential selective advantages of parasite localization to adipose tissue have been proposed, including ease of transmission, relative shelter from the immune system, and/or the presence of abundant energy stores during fasting. Nonetheless, the biological significance of sequestration in adipose on the host response to parasite infection, if any, remains unknown.

The major finding here is that CD36-dependent sequestration of *Pb*A-infected RBCs in WAT of C57BL/6 mice correlated with an increase in the circulating adipokine leptin. In each model tested, including three parasite variants that failed to sequester in adipose tissue, and in both sexes of CD36KO mice that fail to support adipose sequestration, leptin levels were reduced. The same was not true of the other major CD36-dependent sequestering tissue, lung. Circulating leptin levels failed to correlate with *Pb*A levels in this tissue, although whether the observed luciferase activity represented iRBC cytoadherence or accumulation following vascular damage/occlusion was not addressed in this study. Also relevant is the consistent correlation found between WAT parasite sequestration and brain parasite accumulation/sequestration in both experimental and human CM, with the specific exception of CD36KO female mice (discussed in greater detail below). Combined with our previous finding that increased leptin during blood-stage *Pb*A infection in mice is required for maximum penetrance of ECM neuropathology (*33*), these data support a model in which sequestration of iRBCs specifically in WAT contributes to ECM neuropathology likely through effects on vascular and immune activation. While WAT is the largest endocrine organ, where adipocytes are a major source of leptin under homeostatic conditions, other cell types can also produce leptin, and thus, whether WAT is the sole source of leptin or other proinflammatory cytokines relevant to ECM pathology remains a limitation of the current study.

Mechanistically, our data point to a role for mTORC1 activation in increased leptin expression in WAT in vivo. Treatment with rapamycin, a U.S. Food and Drug Administration (FDA)–approved mTORC1 inhibitor, significantly reduced serum leptin levels and protected mice from ECM even after a single dose injected late in infection. These data are consistent with previous reports showing decreased circulating leptin levels upon rapamycin treatment in mice and humans (*40*). While our data in cultured adipocytes supports cell-autonomous regulation of leptin expression by mTORC1 signaling, the pleiotropic effects of rapamycin in vivo on T cell migration, vascular activation, and parasite sequestration make it difficult to unravel the specific mechanism underlying reduced leptin expression. Nonetheless, these findings build on previous reports (*33*, *41*, *42*), highlighting the therapeutic potential of rapamycin to protect against CM by targeting different cell types and inhibiting multiple mechanisms of disease.

A further limitation of the study is that we do not know the mechanism by which mTORC1 is activated in adipocytes upon cytoadherence of iRBCs to CD36-expressing endothelial cells. However, failure to find schizonts outside of the adipose tissue microvasculature combined with evidence of vascular permeability suggests that leakage of parasite material upon iRBC lysis is at least one mechanism allowing parasite-induced adipocyte mTORC1 activation and increased leptin expression. Last, our data point to conservation of this phenomenon in *P. falciparum*–induced pediatric CM, based on the increase in leptin expression and phosphorylation of markers of mTORC1 activity in adipocytes in postmortem adipose samples. A schematic model of the cellular and molecular mechanisms by which specific parasite sequestration in WAT contributes to neuropathology in CM is presented in Fig. 5.

The biological significance of CD36-mediated sequestration in neuropathology of both ECM and CM remains unclear. Human genetic studies of CD36 deficiency have yielded conflicting results, associating with higher susceptibility to severe and/or CM in some studies (*43*, *44*) but protection in others (*45*–*47*). CD36 is expressed only at very low levels in brain vasculature, and most *P. falciparum* isolates obtained from infected individuals bind to CD36 regardless of the severity of the infection (*48*). CD36 is highly expressed in tissues involved in fatty acid metabolism but is not up-regulated by proinflammatory cytokines associated with fatal malaria (*49*). In rodents, the finding that iRBC sequestration is dissociable from ECM pathology in CD36KO mice led to the conclusion that CD36-mediated sequestration in peripheral organs is not the basis of ECM (*24*), a phenotype confirmed here. Also consistent with this conclusion are reports that some nonsequestering *Pb*K173 strains can still cause ECM (*11*, *50*, *51*).

The unexpected finding here that ECM susceptibility in CD36KO mice was a sexual dimorphic trait, while failure to support sequestration was not, complicates the interpretation that CD36-dependent sequestration is not the basis for ECM (*11*, *24*). The finding is unexpected for two reasons: first, because ECM in WT mice occurs in both sexes without significant sexual dimorphism as reported here and elsewhere, and second, because although the original studies reported only female CD36KO mice (*24*, *25*), another study reported a similar phenotype in CD36KO males with the caveat that all animals were lethally irradiated followed by bone marrow reconstitution to study the role of CD36 in hematopoietic versus nonhematopoietic cells (*52*).

With respect to the potential biological importance of sequestration in ECM, while it is possible that ECM is unrelated to CD36-dependent adipose sequestration, alternately, there may exist sexually dimorphic traits in female CD36KO mice that bypass a requirement for adipose sequestration specifically in this mutant. Differences in leptin signaling may be one such trait. In one report, CD36KO mice had ~2.5-fold elevated circulating leptin relative to WT mice due to loss of fatty acid uptake that normally inhibits leptin secretion by adipocytes, with females 40% higher than males (*53*). Here, we failed to see a significant increase in leptin in CD36KO mice but instead observed sexual dimorphism in baseline levels (reduced in females) and in the response to *Pb*A infection (reduced at day 6 versus day 0 in males). Changes in leptin sensitivity in the absence of CD36 may also play a role (*53*–*56*). A number of other possibilities also exist, as CD36 is a major fatty acid translocase important in endothelial cells and parenchymal cells particularly in adipose and muscle under conditions of low free fatty acids availability (*57*) and is also associated with insulin resistance and inflammation, in part, via its role in uptake of oxidized low-density lipoprotein (LDL) by macrophages. Unfortunately, although a number of additional phenotypes of CD36KO mice have been reported, including resistance to weight gain on high-fat diet and a reduction in another adipokine, adiponectin, many studies only report the results of one sex, and thus, sexual dimorphisms are difficult to assess. At the molecular level, our study is hampered by the demonstration of reduced WAT mTORC1 activation only in male CD36KO mice. However, both the proposed trigger and functional result of mTORC1 activation, notably parasite sequestration and leptin production, respectively, are significantly reduced in CD36KO females and males relative to WT mice, strongly suggesting similar mTORC1 activation status upon

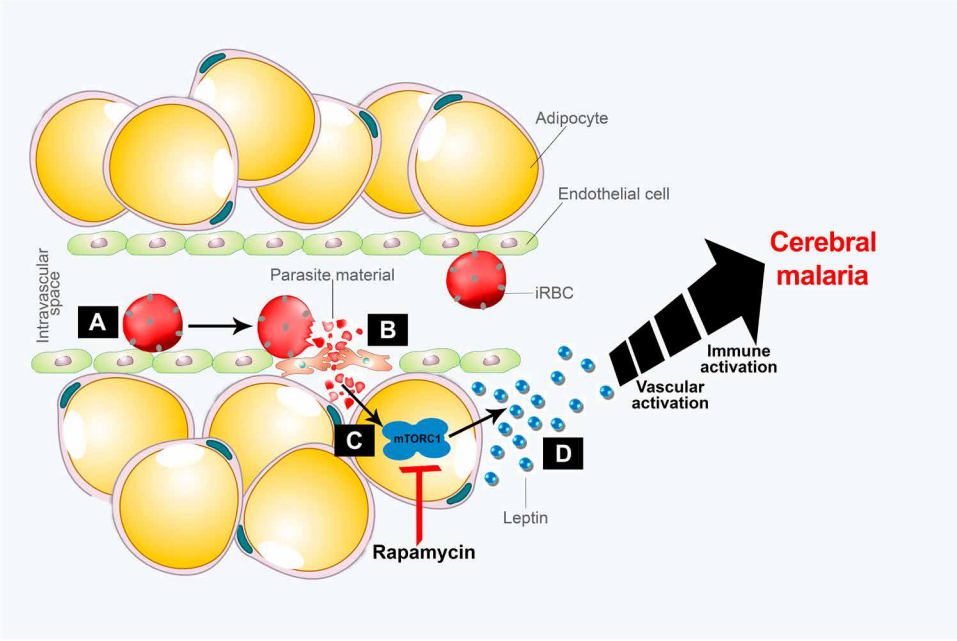


**Fig. 5. Model for the role of WAT iRBC sequestration in the neuropathology of CM.** (**A** to **C**) CD36-dependent adhesion of infected RBCs to WAT endothelium (A) results in local vascular permeability potentially allowing contact between parasite material and adipocytes (B) and subsequent mTORC1 activation in these cells (C). (**D**) mTORC1 activation triggers the local expression and production of adipocyte-derived leptin. Circulating leptin increases upon infection and is required for full penetrance of neuropathology and mortality in the ECM model. Rapamycin treatment suppresses mTORC1 activation in WAT, reduces circulating leptin, and protects against neuropathology. In humans, although *P. falciparum* infection does not increase circulating leptin levels, iRBC sequestration, tissue leptin expression, and mTORC1 activity are positively correlated with CM in ScWAT.

infection in both sexes. Future studies are thus required to determine the mechanism of differential susceptibility to ECM between male and female CD36KO mice, which may shed further light on the uncertain role of CD36-mediated sequestration of WAT in cerebral complications of malarial infection. Notably, although the effect of rapamycin is also known to be affected by sex in other contexts, in our multiple experiments, we have not identified any sexual dimorphism in response to rapamycin treatment in terms of parasitemia and survival in WT mice.

Our data fail to support a role for increased circulating leptin in neuropathology of pediatric CM and thus merit caution with regard to extrapolation from ECM to CM regarding the importance of WAT sequestration. Nonetheless, the conservation of iRBC sequestration, mTORC1 activation, and increased local leptin expression in WAT in both humans and mice observed here remain suggestive of potential disease relevance, either functionally for the parasite or the host response or as a marker that could be exploited for therapeutic purposes. Species-specific differences in effects of iRBC WAT sequestration on circulating leptin could be related to the observation that WAT sequestration in humans appears to be limited to specific depots (*2*), while in mice sequestration in visceral fat was abundant and thus likely to contribute significantly to circulating leptin levels. Because adipocytes are found in intimate contact with secondary lymphoid organs, vasculature, and neuro-adipose junctions (*58*), it is also possible that local leptin production could exert pathogenic effects in a paracrine manner, similar to the effects of perivascular WAT-derived adipokines on cardiovascular disease (*59*). Last, total leptin activity rather than its circulating levels alone might be the most relevant diagnostic factor in the pathology of human CM. The soluble leptin receptor reflects total activity of leptin, and hence, future studies may determine how the ratio between leptin and its soluble receptor predicts the pathogenesis and outcome of human CM. Another adipokine, adiponectin, has anti-inflammatory properties that could counterbalance the proinflammatory effects of leptin and influence the course of acute inflammation. Further research is warranted to elucidate a role for leptin/leptin receptor and leptin/adiponectin ratios in human CM pathology and their value as prognosis and/or diagnosis biomarkers. Moreover, if confirmed, the establishment of these ratios as pathogenic factors in the development of CM could open previously unidentified avenues for therapeutic interventions.

Notably, consistent with a potential role of ScWAT in disease progression, it has been shown in postmortem studies of CM cases that endothelial cells obtained from ScWAT are similar to endothelial cells from cerebral vasculature in features relevant to CM pathology such as tumor necrosis factor–α (TNF-α)–induced expression of adhesion molecules (*8*). Future experiments are thus required to uncover mechanisms of depot-specific WAT sequestration in humans and its relationship with disease severity.

WAT is the largest endocrine organ in the mammalian body, and this study suggests its importance in the pathogenic consequences of malarial infection. Furthermore, our data suggest targeting ScWAT sequestration and/or leptin production, for example, with mTORC1 inhibitors such as the FDA-approved drug rapamycin, as potential new avenues for CM treatment. Last, the apparent specificity of ScWAT sequestration in CM patients and the relative accessibility of this tissue suggest potential diagnostic opportunities for the determination of CM severity and prognosis.

## MATERIALS AND METHODS

### Human plasma and WAT samples

Archived samples in this study were part of larger studies assessing long-term neurocognitive outcomes, pathology, and inflammatory markers in children with CM and severe malarial anemia (SMA).

#### *French, Senegalese, and Cambodian samples*

*P. falciparum*–infected children aged less than 4 years were enrolled with a Blantyre coma score of <2 persisting for 30 min and/or at least two seizure episodes within 24 hours, with no other obvious causes of coma. Lumbar puncture was systematically performed to exclude meningitis. Children were given the appropriate treatment, as recommended by the local Ministry of Public Health. Controls consisted of plasma samples from healthy French Caucasian blood donors and malaria-negative Senegalese volunteers.

#### *Uganda samples*

Children with CM between 18 months and 12 years of age were enrolled. CM was defined as (i) coma (Blantyre Coma Scale score ≤ 2 in children ≤5 years or Glasgow Coma Scale score ≤ 8 in children >5 years), (ii) *P. falciparum* on blood smear, and (iii) no other known cause of coma (e.g., meningitis or encephalitis). Children with CM were managed according to the local Ministry of Health treatment guidelines at the time of the study. Children with CM were assessed for malaria retinopathy by indirect ophthalmoscopy. SMA was defined as either a hemoglobin level of <5 g/dl or a hematocrit of <15%. Controls consisted of malaria-negative and asymptomatic malaria-positive Uganda samples.

#### *Malawi samples*

Children aged 6 months to 9 years who satisfied the clinical case definition of CM were enrolled in the study after consent was obtained from a parent or guardian. CM was defined as a Blantyre Coma Score of ≤2, peripheral parasitemia with *P. falciparum* of any density, and no other discernible causes of coma.

Subcutaneous WAT tissue samples were cut from blocks generated as part of an existing project involving patients with pediatric CM from Malawi (*15*). Uninfected controls were obtained from discarded tissue following vascular surgery.

### Mice

All experimental mice were 8 to 10 weeks of age. WT female and male C57BL/6 (000664) mice on a C57BL/6 background were purchased from The Jackson Laboratory (Bar Harbor, ME). Male and female CD36KO mice on a C57BL/6 background were either purchased directly from The Jackson Laboratory (019006) or bred from heterozygous animals in our facility. Transgenic UBC-GFP C57B/6 mice were obtained from the Institute of Cell Biology, University of Bern, Switzerland. Animals were housed four to five per cage and kept under standard laboratory conditions and allowed free access to water and food at all times. All experiments were performed with the approval of the appropriate institutional animal care and use committee associated with Harvard Medical Area, University of Glasgow, or University of Bern.

### Parasites and infections

All four parasite strains used, including *Pb*A, ΔSMAC, ΔSBP1 (*34*, *35*), and *Pb*K173 (*36*), were transgenic for constitutive expression of GFP-luciferase. In some sequestration experiments, mCherry-expressing *Pb*A parasites (line 1804 mCherry$_{Hsp70}$ from the *Pb*A GIMO mother line 1596cl1, Leiden) were used. For infections, cryopreserved parasites were thawed and passaged once in vivo before being used to infect experimental mice with 0.5 million parasitized RBCs per mouse by tail vein injection. When *Pb*ΔSMAC or ΔSBP1 parasites were used for infections, their respective parental WT lines were used as controls. Parasites from peripheral blood were stained with SYTO16, and the percentage of infected cells was calculated by flow cytometry (*60*). Survival was followed for up to day 12.

### Parasite sequestration

Infected mice were sacrificed on the indicated day and perfused with cold phosphate-buffered saline (PBS) intracardially. The organs were harvested, weighed, and homogenized in an equal volume per milligram of tissue of luciferase activity assay buffer (Invitrogen). Equal volumes were mixed with luciferin substrate and measured in a 96-well luminometer (Biotek Synergy 2). For in vivo imaging, infected mice were anesthetized and injected with luciferin. Luciferase activity was detected with IVIS Lumina In Vivo Imaging System.

### Rapamycin treatment

Mice were treated with vehicle (5% Tween/5% polyethylene glycol 400) or rapamycin (1 mg/kg) (LC Laboratories, Woburn, MA) once by intraperitoneal injection.

### ELISA measurements

Mouse serum leptin was measured using a commercial enzyme-linked immunosorbent assay (ELISA) kit from Millipore (EZML-82 K; 0.2 to 30 ng/ml), following the manufacturer's instructions. Undiluted serum (5 μl) was used per assay. Human leptin was measured using the Human Leptin Quantikine ELISA Kit from R&D Systems (DLP00, 15.6 to 1000 pg/ml). Plasma (5 μl) diluted 1:10 in dilution buffer provided by the manufacturer (50 μl total) was used per reaction. Adiponectin and leptin were measured from supernatants of cultured differentiated primary adipocytes using the commercial mouse ELISA kits from R&D Systems (adiponectin, MRP300; 0.2 to 10 ng/ml).

### Western blotting

NP-40 extracts of snap-frozen adipose tissues were separated by SDS–polyacrylamide gel electrophoresis, transferred to polyvinylidene difluoride membranes (Millipore), and stained with the following anti bodies (Cell Signaling Technology, Beverly, MA) at a 1:1000 dilution: rabbit (Rb) anti–β-actin, Rb anti-total p70 S6K, and Rb anti–phospho-p70 S6K (Thr$^{389}$). After washing in PBS + Tween 20, membranes were incubated with horseradish peroxidase–conjugated antibodies 1:5000 diluted in 5% skim milk. Detection was performed using the SuperSignal West Femto substrate (Thermo Fisher Scientific).

### Microscopy

Sections were cut from paraffinized mouse organs from PBS-perfused animals or from human adipose samples and placed on slides. Antigen retrieval was performed by immersing the slides in 98.5°C prewarmed universal antigen retrieval solution (R&D Systems). After cooling in PBS, slides were permeabilized in 0.25% Triton X-100 in PBS, followed by blocking in a 10% normal goat serum solution supplemented with 0.2 M glycine and 1% bovine serum albumin. Primary staining was performed with anti-leptin rabbit polyclonal (Abcam, ab16227) or anti–phospho-Ser$^{235/235}$ S6 Alexa Fluor 488–conjugated rabbit monoclonal (Cell Signaling Technology, 4803) diluted 1:200 in blocking solution. Mouse and human WAT leptin and pS6 images were obtained in a Nikon TiE inverted microscope adapted with a Yokogawa CSU-X1 spinning disc processor and an air Plan Apo 20× (numerical aperture = 0.75). For image analysis, each individual image

file was processed independently. No color or balance adjustment was performed on any image. For quantification, a threshold was defined using a positive and negative control. Then, the same threshold was used in a given cohort to measure fluorescence intensity and area of expression. To ensure unbiased quantification, the experiment was blinded as follows. After staining, slides were renumbered before acquisition and scanned by a different investigator. Image files were then quantified blindly by a third investigator before decoding.

ScWAT H&E images were acquired on a Zeiss Axio observer with a Plan apochromatic 20×/0.8 M27 [free working distance = 0.55] high-performance objective and an Axiocam 702 mono (D) high-performance monochromatic camera using Zen software. Images of mCherry-expressing *PbA* in iRBCs sequestered in microvasculature of UBC-GFP C57BL/6 pgWAT were acquired using a Zeiss spinning disc confocal microscope, with a Yokogawa CSU-X1 processor and a water immersion 63× objective. For dextran imaging, C57BL/6 mice were intravenously injected with 200 µl of fluorescein isothiocyanate (FITC)–dextran (5 mg/ml) (70 kDa), and the adipose tissue was imaged within 10 min after injection. Images were acquired using a Zeiss spinning disc confocal microscope, with a Yokogawa CSU-X1 processor and a water immersion 63× objective.

### In vitro experiments

Primary mouse preadipocytes were differentiated as follows: After confluence, cells were incubated with a cocktail containing dexamethasone (2.5 µM), 3-isobutyl-1-methylantine (0.5 mM), and insulin (10 µg/ml) for 2 days. The medium was then changed every 2 days until complete cell bubbling was observed. Differentiated primary adipocytes were then infected with lentivirus expressing an shRNA targeting the mTORC1 inhibitory protein TSC2 or a scrambled shRNA. Two days after infection, the medium was removed for leptin and adiponectin detection by ELISA, and cells were lysed using TRIzol for reverse transcription quantitative polymerase chain reaction (RT-qPCR) analysis of leptin and adiponectin transcripts.

### Gene expression

Total RNA was extracted from cultured cells using TRIzol (Invitrogen). Hexamer-primed complementary DNA (cDNA) was synthesized with the Verso cDNA Kit (Thermo Fisher Scientific) according to the manufacturer's instructions. Quantitative real-time polymerase chain reaction was performed with MyIQ (Bio-Rad) using SYBR Green. Relative expression was calculated with the $\Delta\Delta C_t$ method. cDNA expression of each sample was standardized to RPLA13. Each sample was tested in duplicate at least twice. Primer sequences used are as follows: leptin, 5′-GAGACCCCTGTGTCGGTTC-3′ (forward) and 5′-CTGCGTGTGTGAAATGTCATTG-3′ (reverse); adiponectin, 5′-TGTTCCTCTTAATCCTGCCCA-3′ (forward) and 5′-CCAACCTGCACAAGTTCCCTT-3′ (reverse).

### Statistics

Data are expressed as mean ± SD. Statistical analyses were performed in GraphPad Prism, and a $P$ value of less than 0.05 was considered significant.

View/request a protocol for this paper from *Bio-protocol*.

## REFERENCES AND NOTES


1. K. Dorovini-Zis, K. Schmidt, H. Huynh, W. Fu, R. O. Whitten, D. Milner, S. Kamiza, M. Molyneux, T. E. Taylor, The neuropathology of fatal cerebral malaria in Malawian children. *Am. J. Pathol.* **178**, 2146–2158 (2011).
2. D. A. Milner Jr., R. O. Whitten, S. Kamiza, R. Carr, G. Liomba, C. Dzamalala, K. B. Seydel, M. E. Molyneux, T. E. Taylor, The systemic pathology of cerebral malaria in African children. *Front. Cell. Infect. Microbiol.* **4**, 104 (2014).
3. K. B. Seydel, S. D. Kampondeni, C. Valim, M. J. Potchen, D. A. Milner, F. W. Muwalo, G. L. Birbeck, W. G. Bradley, L. L. Fox, S. J. Glover, C. A. Hammond, R. S. Heyderman, C. A. Chilingulo, M. E. Molyneux, T. E. Taylor, Brain swelling and death in children with cerebral malaria. *N. Engl. J. Med.* **372**, 1126–1137 (2015).
4. S. S. Struik, E. M. Riley, Does malaria suffer from lack of memory? *Immunol. Rev.* **201**, 268–290 (2004).
5. H. C. van der Heyde, J. Nolan, V. Combes, I. Gramaglia, G. E. Grau, A unified hypothesis for the genesis of cerebral malaria: Sequestration, inflammation and hemostasis leading to microcirculatory dysfunction. *Trends Parasitol.* **22**, 503–508 (2006).
6. G. E. Grau, P. F. Piguet, P. Vassalli, P. H. Lambert, Tumor-necrosis factor and other cytokines in cerebral malaria: Experimental and clinical data. *Immunol. Rev.* **112**, 49–70 (1989).
7. I. A. Clark, K. A. Rockett, The cytokine theory of human cerebral malaria. *Parasitol. Today* **10**, 410–412 (1994).
8. S. C. Wassmer, C. A. Moxon, T. Taylor, G. E. Grau, M. E. Molyneux, A. G. Craig, Vascular endothelial cells cultured from patients with cerebral or uncomplicated malaria exhibit differential reactivity to TNF. *Cell. Microbiol.* **13**, 198–209 (2011).
9. G. E. Grau, C. D. Mackenzie, R. A. Carr, M. Redard, G. Pizzolato, C. Allasia, C. Cataldo, T. E. Taylor, M. E. Molyneux, Platelet accumulation in brain microvessels in fatal pediatric cerebral malaria. *J. Infect. Dis.* **187**, 461–466 (2003).
10. C. A. Moxon, R. S. Heyderman, S. C. Wassmer, Dysregulation of coagulation in cerebral malaria. *Mol. Biochem. Parasitol.* **166**, 99–108 (2009).
11. B. Franke-Fayard, J. Fonager, A. Braks, S. M. Khan, C. J. Janse, Sequestration and tissue accumulation of human malaria parasites: Can we learn anything from rodent models of malaria? *PLOS Pathog.* **6**, e1001032 (2010).
12. M. Aikawa, J. W. Barnwell, M. M. Oo, M. Iseki, D. Taylor, R. J. Howard, The pathology of human cerebral malaria. *Am. J. Trop. Med. Hyg.* **43**, 30–37 (1990).
13. E. Pongponratn, G. D. H. Turner, N. P. J. Day, N. H. Phu, J. A. Simpson, K. Stepniewska, N. T. H. Mai, P. Viriyavejakul, S. Looareesuwan, T. T. Hien, D. J. P. Ferguson, N. J. White, An ultrastructural study of the brain in fatal *Plasmodium falciparum* malaria. *Am. J. Trop. Med. Hyg.* **69**, 345–359 (2003).
14. T. E. Taylor, W. J. Fu, R. A. Carr, R. O. Whitten, J. G. Mueller, N. G. Fosiko, S. Lewallen, N. G. Liomba, M. E. Molyneux, Differentiating the pathologies of cerebral malaria by postmortem parasite counts. *Nat. Med.* **10**, 143–145 (2004).
15. D. A. Milner Jr., J. J. Lee, C. Frantzreb, R. O. Whitten, S. Kamiza, R. A. Carr, A. Pradham, R. E. Factor, K. Playforth, G. Liomba, C. Dzamalala, K. B. Seydel, M. E. Molyneux, T. E. Taylor, Quantitative assessment of multiorgan sequestration of parasites in fatal pediatric cerebral malaria. *J. Infect. Dis.* **212**, 1317–1321 (2015).
16. K. B. Seydel, D. A. Milner Jr., S. B. Kamiza, M. E. Molyneux, T. E. Taylor, The distribution and intensity of parasite sequestration in comatose Malawian children. *J. Infect. Dis.* **194**, 208–215 (2006).
17. J. D. Smith, C. E. Chitnis, A. G. Craig, D. J. Roberts, D. E. Hudson-Taylor, D. S. Peterson, R. Pinches, C. I. Newbold, L. H. Miller, Switches in expression of *Plasmodium falciparum* var genes correlate with changes in antigenic and cytoadherent phenotypes of infected erythrocytes. *Cell* **82**, 101–110 (1995).
18. S. M. Kraemer, J. D. Smith, A family affair: *var* genes, PfEMP1 binding, and malaria disease. *Curr. Opin. Microbiol.* **9**, 374–380 (2006).
19. J. A. Rowe, A. Claessens, R. A. Corrigan, M. Arman, Adhesion of *Plasmodium falciparum*-infected erythrocytes to human cells: Molecular mechanisms and therapeutic implications. *Expert Rev. Mol. Med.* **11**, e16 (2009).
20. L. Turner, T. Lavstsen, S. S. Berger, C. W. Wang, J. E. V. Petersen, M. Avril, A. J. Brazier, J. Freeth, J. S. Jespersen, M. A. Nielsen, P. Magistrado, J. Lusingu, J. D. Smith, M. K. Higgins, T. G. Theander, Severe malaria is associated with parasite binding to endothelial protein C receptor. *Nature* **498**, 502–505 (2013).
21. A. Cabrera, D. Neculai, K. C. Kain, CD36 and malaria: Friends or foes? A decade of data provides some answers. *Trends Parasitol.* **30**, 436–444 (2014).
22. D. A. Cunningham, J. W. Lin, T. Brugat, W. Jarra, I. Tumwine, G. Kushinga, J. Ramesar, B. Franke-Fayard, J. Langhorne, ICAM-1 is a key receptor mediating cytoadherence and pathology in the *Plasmodium chabaudi* malaria model. *Malar. J.* **16**, 185 (2017).
23. R. L. Silverstein, M. Febbraio, CD36, a scavenger receptor involved in immunity, metabolism, angiogenesis, and behavior. *Sci. Signal.* **2**, re3 (2009).
24. B. Franke-Fayard, C. J. Janse, M. Cunha-Rodrigues, J. Ramesar, P. Buscher, I. Que, C. Lowik, P. J. Voshol, M. A. M. den Boer, S. G. van Duinen, M. Febbraio, M. M. Mota, A. P. Waters, Murine malaria parasite sequestration: CD36 is the major receptor, but cerebral pathology is unlinked to sequestration. *Proc. Natl. Acad. Sci. U.S.A.* **102**, 11468–11473 (2005).
25. F. E. Lovegrove, S. A. Gharib, L. Peña-Castillo, S. N. Patel, J. T. Ruzinski, T. R. Hughes, W. C. Liles, K. C. Kain, Parasite burden and CD36-mediated sequestration are determinants of acute lung injury in an experimental malaria model. *PLOS Pathog.* **4**, e1000068 (2008).

26. F. El-Assaad, J. Wheway, A. J. Mitchell, J. Lou, N. H. Hunt, V. Combes, G. E. R. Grau, Cytoadherence of *Plasmodium berghei*-infected red blood cells to murine brain and lung microvascular endothelial cells in vitro. *Infect. Immun.* **81**, 3984–3991 (2013).
27. H. Tilg, A. R. Moschen, Adipocytokines: Mediators linking adipose tissue, inflammation and immunity. *Nat. Rev. Immunol.* **6**, 772–783 (2006).
28. A. Schaffler, J. Scholmerich, Innate immunity and adipose tissue biology. *Trends Immunol.* **31**, 228–235 (2010).
29. N. Iikuni, Q. L. Lam, L. Lu, G. Matarese, A. La Cava, Leptin and inflammation. *Curr. Immunol. Rev.* **4**, 70–79 (2008).
30. A. Bouloumie, T. Marumo, M. Lafontan, R. Busse, Leptin induces oxidative stress in human endothelial cells. *FASEB J.* **13**, 1231–1238 (1999).
31. M. Korda, R. Kubant, S. Patton, T. Malinski, Leptin-induced endothelial dysfunction in obesity. *Am. J. Physiol. Heart Circ. Physiol.* **295**, H1514–H1521 (2008).
32. M. Pulido-Mendez, J. De Sanctis, A. Rodriguez-Acosta, Leptin and leptin receptors during malaria infection in mice. *Folia Parasitol.* **49**, 249–251 (2002).
33. P. Mejia, J. H. Treviño-Villarreal, C. Hine, E. Harputlugil, S. Lang, E. Calay, R. Rogers, D. Wirth, M. T. Duraisingh, J. R. Mitchell, Dietary restriction protects against experimental cerebral malaria via leptin modulation and T-cell mTORC1 suppression. *Nat. Commun.* **6**, 6050 (2015).
34. J. Fonager, E. M. Pasini, J. A. M. Braks, O. Klop, J. Ramesar, E. J. Remarque, I. O. C. M. Vroegrijk, S. G. van Duinen, A. W. Thomas, S. M. Khan, M. Mann, C. H. M. Kocken, C. J. Janse, B. M. D. Franke-Fayard, Reduced CD36-dependent tissue sequestration of *Plasmodium*-infected erythrocytes is detrimental to malaria parasite growth in vivo. *J. Exp. Med.* **209**, 93–107 (2012).
35. M. De Niz, A.-K. Ullrich, A. Heiber, A. B. Soares, C. Pick, R. Lyck, D. Keller, G. Kaiser, M. Prado, S. Flemming, H. D. Portillo, C. J. Janse, V. Heussler, T. Spielmann, The machinery underlying malaria parasite virulence is conserved between rodent and human malaria parasites. *Nat. Commun.* **7**, 11659 (2016).
36. L. Rodrigues-Duarte, L. de Moraes, R. Barboza, C. R. F. Marinho, B. Franke-Fayard, C. J. Janse, C. Penha-Gonçalves, Distinct placental malaria pathology caused by different *Plasmodium berghei* lines that fail to induce cerebral malaria in the C57BL/6 mouse. *Malar. J.* **11**, 231 (2012).
37. C. Roh, J. Han, A. Tzatsos, K. V. Kandror, Nutrient-sensing mTOR-mediated pathway regulates leptin production in isolated rat adipocytes. *Am. J. Physiol. Endocrinol. Metab.* **284**, E322–E330 (2003).
38. R. S. Desowitz, L. H. Miller, R. D. Buchanan, B. Permpanich, The sites of deep vascular schizogony in *Plasmodium coatneyi* malaria. *Trans. R. Soc. Trop. Med. Hyg.* **63**, 198–202 (1969).
39. H. B. Tanowitz, P. E. Scherer, M. M. Mota, L. M. Figueiredo, Adipose tissue: A safe haven for parasites? *Trends Parasitol.* **33**, 276–284 (2017).
40. G. R. Chang, Y. S. Chiu, Y. Y. Wu, W. Y. Chen, J. W. Liao, T. H. Chao, F. C. Mao, Rapamycin protects against high fat diet-induced obesity in C57BL/6J mice. *J. Pharmacol. Sci.* **109**, 496–503 (2009).
41. E. B. Gordon, G. T. Hart, T. M. Tran, M. Waisberg, M. Akkaya, J. Skinner, S. Zinöcker, M. Pena, T. Yazew, C.-F. Qi, L. H. Miller, S. K. Pierce, Inhibiting the Mammalian target of rapamycin blocks the development of experimental cerebral malaria. *mBio* **6**, e00725 (2015).
42. P. Mejia, J. H. Treviño-Villarreal, J. S. Reynolds, M. de Niz, A. Thompson, M. Marti, J. R. Mitchell, A single rapamycin dose protects against late-stage experimental cerebral malaria via modulation of host immunity, endothelial activation and parasite sequestration. *Malar. J.* **16**, 455 (2017).
43. G. Ayodo, A. L. Price, A. Keinan, A. Ajwang, M. F. Otieno, A. S. S. Orago, N. Patterson, D. Reich, Combining evidence of natural selection with association analysis increases power to detect malaria-resistance variants. *Am. J. Hum. Genet.* **81**, 234–242 (2007).
44. T. J. Aitman, L. D. Cooper, P. J. Norsworthy, F. N. Wahid, J. K. Gray, B. R. Curtis, P. M. McKeigue, D. Kwiatkowski, B. M. Greenwood, R. W. Snow, A. V. Hill, J. Scott, Malaria susceptibility and CD36 mutation. *Nature* **405**, 1015–1016 (2000).
45. A. Pain, B. C. Urban, O. Kai, C. Casals-Pascual, J. Shafi, K. Marsh, D. J. Roberts, A non-sense mutation in Cd36 gene is associated with protection from severe malaria. *Lancet* **357**, 1502–1503 (2001).
46. A. Das, T. K. Das, U. Sahu, B. P. Das, S. K. Kar, M. R. Ranjit, CD36 T188G gene polymorphism and severe falciparum malaria in India. *Trans. R. Soc. Trop. Med. Hyg.* **103**, 687–690 (2009).
47. S. Sinha, T. Qidwai, K. Kanchan, P. Anand, G. N. Jha, S. S. Pati, S. Mohanty, S. K. Mishra, P. K. Tyagi, S. K. Sharma; Indian Genome Variation Consortium, V. Venkatesh, S. Habib, Variations in host genes encoding adhesion molecules and susceptibility to falciparum malaria in India. *Malar. J.* **7**, 250 (2008).
48. C. Newbold, P. Warn, G. Black, A. Berendt, A. Craig, B. Snow, M. Msobo, N. Peshu, K. Marsh, Receptor-specific adhesion and clinical disease in *Plasmodium falciparum*. *Am. J. Trop. Med. Hyg.* **57**, 389–398 (1997).
49. A. R. Berendt, D. L. Simmons, J. Tansey, C. I. Newbold, K. Marsh, Intercellular adhesion molecule-1 is an endothelial cell adhesion receptor for *Plasmodium falciparum*. *Nature* **341**, 57–59 (1989).
50. J. H. Curfs, J. W. van der Meer, R. W. Sauerwein, W. M. Eling, Low dosages of interleukin 1 protect mice against lethal cerebral malaria. *J. Exp. Med.* **172**, 1287–1291 (1990).
51. C. C. Hermsen, E. Mommers, T. van de Wiel, R. W. Sauerwein, W. M. Eling, Convulsions due to increased permeability of the blood-brain barrier in experimental cerebral malaria can be prevented by splenectomy or anti-T cell treatment. *J. Infect. Dis.* **178**, 1225–1227 (1998).
52. M. Cunha-Rodrigues, S. Portugal, M. Febbraio, M. M. Mota, Bone marrow chimeric mice reveal a dual role for CD36 in *Plasmodium berghei* ANKA infection. *Malar. J.* **6**, 32 (2007).
53. T. Hajri, A. M. Hall, D. R. Jensen, T. A. Pietka, V. A. Drover, H. Tao, R. Eckel, N. A. Abumrad, CD36-facilitated fatty acid uptake inhibits leptin production and signaling in adipose tissue. *Diabetes* **56**, 1872–1880 (2007).
54. C. Bjørbaek, B. B. Kahn, Leptin signaling in the central nervous system and the periphery. *Recent Prog. Horm. Res.* **59**, 305–331 (2004).
55. S. H. Bates, W. H. Stearns, T. A. Dundon, M. Schubert, A. W. K. Tso, Y. Wang, A. S. Banks, H. J. Lavery, A. K. Haq, E. Maratos-Flier, B. G. Neel, M. W. Schwartz, M. G. Myers Jr., STAT3 signalling is required for leptin regulation of energy balance but not reproduction. *Nature* **421**, 856–859 (2003).
56. C. Buettner, A. Pocai, E. D. Muse, A. M. Etgen, M. G. Myers Jr., L. Rossetti, Critical role of STAT3 in leptin's metabolic actions. *Cell Metab.* **4**, 49–60 (2006).
57. N. H. Son, D. Basu, D. Samovski, T. A. Pietka, V. S. Peche, F. Willecke, X. Fang, S. Q. Yu, D. Scerbo, H. R. Chang, F. Sun, S. Bagdasarov, K. Drosatos, S. T. Yeh, A. E. Mullick, K. I. Shoghi, N. Gumaste, K. J. Kim, L. A. Huggins, T. Lhakhang, N. A. Abumrad, I. J. Goldberg, Endothelial cell CD36 optimizes tissue fatty acid uptake. *J. Clin. Invest.* **128**, 4329–4342 (2018).
58. W. Zeng, R. M. Pirzgalska, M. M. A. Pereira, N. Kubasova, A. Barateiro, E. Seixas, Y. H. Lu, A. Kozlova, H. Voss, G. G. Martins, J. M. Friedman, A. I. Domingos, Sympathetic neuro-adipose connections mediate leptin-driven lipolysis. *Cell* **163**, 84–94 (2015).
59. L. Villacorta, L. Chang, The role of perivascular adipose tissue in vasoconstriction, arterial stiffness, and aneurysm. *Horm. Mol. Biol. Clin. Invest.* **21**, 137–147 (2015).
60. M. B. Jiménez-Díaz, T. Mulet, V. Gómez, S. Viera, A. Alvarez, H. Garuti, Y. Vázquez, A. Fernández, J. Ibáñez, M. Jiménez, D. Gargallo-Viola, I. Angulo-Barturen, Quantitative measurement of *Plasmodium*-infected erythrocytes in murine models of malaria by flow cytometry using bidimensional assessment of SYTO-16 fluorescence. *Cytometry A* **75**, 225–235 (2009).


**Acknowledgments:** In memory of James R. Mitchell, an extraordinary mentor, scientist, and friend. **Funding:** M.D.N. was funded by Long-Term EMBO Post-Doctoral Fellowship ALTF 1048-2016. C.C.J. was funded by NIH grant R01 NS055349. The Malawi autopsy study was supported by NIH grant R01AI034969. M.M. was funded by European Research Council consolidator award "BoneMalar". **Author contributions:** P.M., J.H.T.-V., and J.R.M. conceived the study, designed the experiments, and wrote the manuscript. P.M., J.H.T.-V., M.D.N., E.M., A.L., J.S.R., L.B.T., R.O.O., and C.R. performed experiments. T.S., C.K.O., V.T.H., K.B.S., T.E.T., C.C.J., D.A.M., and M.M. provided resources for the study. P.M., J.H.T.-V., M.M., and J.R.M. analyzed the data. All authors read and approved the final manuscript. **Competing interests:** The authors declare that they have no competing interests. **Data and materials availability:** All data needed to evaluate the conclusions in the paper are present in the paper. Additional data related to this paper may be requested from the authors.

Submitted 9 August 2020
Accepted 4 February 2021
Published 24 March 2021
10.1126/sciadv.abe2484

**Citation:** P. Mejia, J. H. Treviño-Villarreal, M. De Niz, E. Meibalan, A. Longchamp, J. S. Reynolds, L. B. Turnbull, R. O. Opoka, C. Roussilhon, T. Spielmann, C. K. Ozaki, V. T. Heussler, K. B. Seydel, T. E. Taylor, C. C. John, D. A. Milner, M. Marti, J. R. Mitchell, Adipose tissue parasite sequestration drives leptin production in mice and correlates with human cerebral malaria. *Sci. Adv.* **7**, eabe2484 (2021).

# Adipose tissue parasite sequestration drives leptin production in mice and correlates with human cerebral malaria

Pedro Mejia, J. Humberto Treviño-Villarreal, Mariana De Niz, Elamaran Meibalan, Alban Longchamp, Justin S. Reynolds, Lindsey B. Turnbull, Robert O. Opoka, Christian Roussilhon, Tobias Spielmann, C. Keith Ozaki, Volker T. Heussler, Karl B. Seydel, Terrie E. Taylor, Chandy C. John, Danny A. Milner, Matthias Marti and James R. Mitchell

*Sci Adv* **7** (13), eabe2484.
DOI: 10.1126/sciadv.abe2484